

# FABRICATION AND CHARACTERIZATION OF SUPERHYDROPHILIC CU MICROPOSTS FOR MICRO HEAT PIPES

Youngsuk Nam and Y. Sungtaek Ju

Mechanical and Aerospace Department, University of California, Los Angeles, USA

**Abstract:** We report fabrication and characterization of multiscale superhydrophilic Cu micropost wicks for potential applications in micro heat pipes. Uniform and nearly defect-free arrays of micro Cu posts with aspect ratios as high as 4 and solid fractions as high as 54% are fabricated over large areas (~3 cm<sup>2</sup>) using electrochemical deposition. The Cu microposts are nanostructured to enhance the wettability of water. The wicking performance of the wicks is characterized using capillary rate of rise experiments. The ratio between the permeability and the effective pore radius, which is a key parameter governing the critical heat flux of micro-heat pipes, is primarily a function of solid fraction for tall posts. The results provide a useful starting point in determining wick parameters to achieve optimal balance between the wicking capability and thermal conductivity.

**Keywords:** Micro heat pipe, Micropost, Wick, Electrochemical deposition

## INTRODUCTION

The thermal management of high-power-density semiconductor devices has been a subject of intense research over the past decades. A number of previous studies reported micro-heat pipes which can be readily integrated into compact electronic systems [1, 2]. The majority of past micro-heat pipes, however, incorporated simple linear grooves, channels, or meshes that offer limited capillary performance as wicks. This led to low heat flux capability, very often below 100 W/cm<sup>2</sup>, and sensitivity to orientation with respect to gravity.

Some recent micro-heat pipes used sintered metal powders to achieve much higher critical heat fluxes [3]. Direct sintering of metal powders, however, is often suited only for heat pipes whose envelopes are made of select ceramics or metals. The effective wick thermal conductivity of sintered powders is also often limited due to small contact areas between spherical powders and heating surfaces.

Another important consideration is a wick material. Copper has been one of the most attractive materials for heat transfer applications due to its high thermal conductivity and favorable processing properties. Poor wettability of water on copper surfaces, however, compromises their phase change heat transfer performance [4-6].

In the present article, we report fabrication and characterization of the capillary performance of wicks that consist of dense arrays of micro Cu posts with aspect ratios as high as 4 and solid fractions as high as 54%. We develop and optimize electroplating and related microfabrication methods to synthesize uniform and nearly defect-free micro-post arrays over areas as large as 3 cm<sup>2</sup>. A controlled chemical oxidation scheme is used to nanostructure the surfaces

of the Cu posts to enhance their wettability. The capillary rate of rise experiments is then used to characterize the wicking performance of the post wicks of various feature sizes.

## EXPERIMENTS

### Electrochemical Deposition of Dense Cu Array

We fabricate dense hexagonal arrays of copper microposts of diameters 30 ~ 100 μm, pitches 65~115 μm, and heights 30 ~ 120 μm using electrochemical deposition. Figure 1 summarizes the process flow.

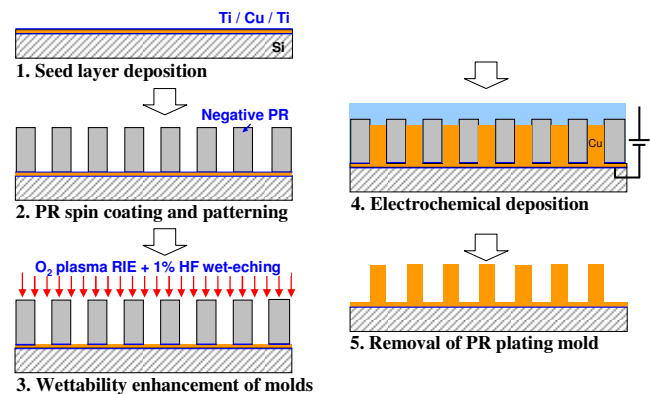


Fig. 1: Process flow for fabricating a copper micropost array.

*Seed layer deposition:* We first deposit a seed layer (Ti/Cu/Ti) on a silicon substrate using e-beam thermal evaporation (CHA Mark 40). The top Ti layer (30 nm) protects the Cu seed layer (350 nm) from oxidation during soft and post bake and oxygen plasma treatment of PR layers.

*PR spin coating and patterning:* A negative PR

layer is spin-coated on the substrate and photolithographically patterned. We choose KMPR® (Microchem, Inc.) rather than more widely used SU-8® as our photoresist as the former can be dissolved in select chemicals, greatly facilitating its removal. To create a mold of thickness over 100  $\mu\text{m}$ , multi-layers of KMPR are spin-coated on the substrate.

*Wettability enhancement of plating molds:* PR-based plating molds are advantageous as they can be readily applied to most common substrates but the plating solution poorly wets the surface of most cured negative photoresists (see Fig. 2(a)). This makes it difficult for electrolytes to penetrate uniformly into deep through-holes, significantly degrading the uniformity of electrochemical deposition.

We subject our molds to oxygen plasma in a commercial reactive ion etching equipment (Technics Fluorine RIE 800, 150 W / 200 mTorr) for 2 ~ 10 min to enhance wettability (Fig. 2). Unlike PDMS [7, 8], the enhanced wettability is maintained for over 24 hours. The slow recovery may be explained by the dense molecular structure of cured PR layers.



Fig. 2: Optical images of droplets (4 $\mu\text{l}$ ) of the electroplating solution on the photoresist layers. (a) before plasma treatment, after 2 min plasma treatment (b) and 10 min treatment (c).

*Electrochemical deposition:* To minimize void formation, which degrades thermal and mechanical properties, a bottom-up plating scheme is used [9, 10]. We find it important to initiate electrochemical deposition using a very low current density ( $\sim 2 \text{ mA/cm}^2$ ). Such a low current density helps mitigate undesired effects of non-uniform current density distributions, which may be caused by residual oxide layers or contamination. Once deposition is activated in all holes, the current density is increased to 7  $\text{mA/cm}^2$  to achieve a higher deposition rate.

*Removal of plating mold:* Removing plating molds is challenging for dense micro-post arrays of high aspect ratios. We use commercially available stripper (Remover PG®) and dissolver (Remover K®, and Neutralizer K®). Figure 3 shows SEM images of final copper micropost arrays fabricated using the

above process.

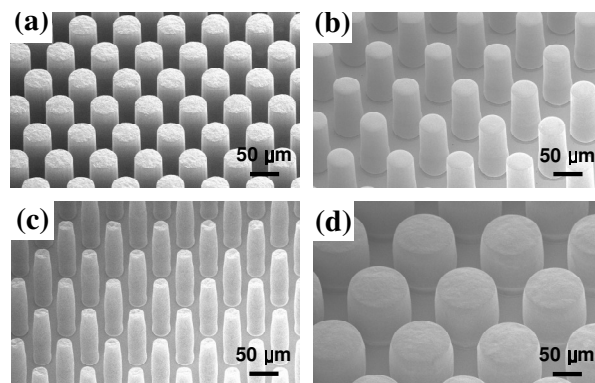


Fig. 3: SEM images of copper micropost arrays fabricated in the present study. Diameter / pitch = (a) 50 / 75, (b) 50 / 100, (c) 30 / 80, (d) 100 / 150 ( $\mu\text{m}$ ).

### Nanostructuring of Cu Surfaces

Controlled chemical oxidation is a convenient way to modify the wettability of Cu surfaces. The unique morphologies and high surface energy of CuO nanostructures allow us to achieve extreme wettability without introducing large parasitic thermal resistance.

Among various possible CuO nanostructures, sharp needle like CuO nanostructures of height approximately 1  $\mu\text{m}$  are chosen based on our previous comparative study [11]. Since the oxidation process is quasi-self limiting, uniform oxide nanostructures can be formed over complex microstructures. The static contact angle of water on flat nanostructured Cu films was measured to be  $< 10^\circ$ .

The nanostructures are formed by immersing the micro-post samples in an alkali solution composed of  $\text{NaClO}_2$ ,  $\text{NaOH}$ ,  $\text{Na}_3\text{PO}_4 \cdot 12\text{H}_2\text{O}$  and DI water. Figure 4(a) confirms that the CuO nanostructures are uniformly formed over the entire surfaces of the Cu microposts. Figure 4 also shows the images of water droplets placed before (b) and after (c) the chemical oxidation. Due to the extreme wettability of the CuO nanostructures, non-wetting copper post wicks are turned into superhydrophilic wicks.

### Capillary Rate of Rise Experiment

The crucial heat flux of micro-heat pipes is most often determined by the capillary performance of their wicks [1, 2]. Many design parameters, such as the post diameter, pitch, pattern, and height, influence the permeability  $K$  and the capillary pressure of micro-post wicks.

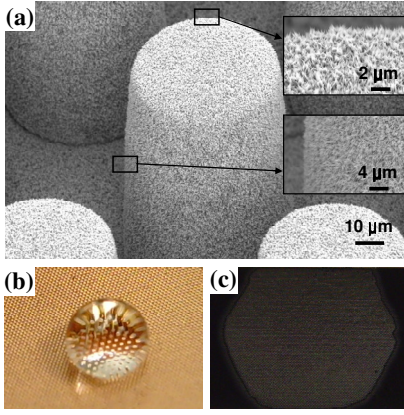


Fig. 4: (a) SEM image of nanostructured Cu microposts. (b-c) Images of 4  $\mu\text{l}$  of water droplets on the bare Cu micropost wick (b) and the nanostructured Cu micro post wick (c).

We use the capillary rate of rise experiments [12, 13] to assess the capillary performance of our micropost wicks. A wick sample (1 cm x 3 cm) is placed perpendicular to the horizontal surface of a liquid reservoir and slowly lowered using a z-stage. Methanol and DI water are used as the test liquid. Once the sample bottom touches the reservoir surface, the liquid rises along the wick via a finite capillary pressure gradient. The location of the rising liquid front is tracked as a function of time using a high speed video camera (Fastcam MC2, Photron) operating at 500 frames per second (fps).

For capillary structures of small effective pore diameters (approximately  $< 300 \mu\text{m}$  for water), the inertia effect is small and the liquid rise is governed by balance among the capillary force, the viscous force, and the gravity:

$$\frac{\sigma_{\text{lg}}}{R_{\text{eff}}} = \frac{\varepsilon}{K} \mu x \frac{dx}{dt} + \rho g x \quad (1)$$

If the gravity effect is negligible, equation 1 reduces to the Washburn's equation [14]:

$$x^2 = (2\sigma\varepsilon\mu)(K/R_{\text{eff}})t \quad (2)$$

Figure 5(a-b) shows selected video frames from one of our capillary rate of rise experiments. When a wick sample touches an open liquid reservoir, a macroscopic side meniscus is first formed. The maximum height of such a meniscus in our samples is measured to be approximately 4 mm for water and 2.5 mm for methanol. These values agree well with the predicted values based on the balance between gravity and capillary force: [15]

$$h_0 = \sqrt{2\sigma/(\rho g)}(1 - \sin \theta_a)^{1/2}, \quad (3)$$

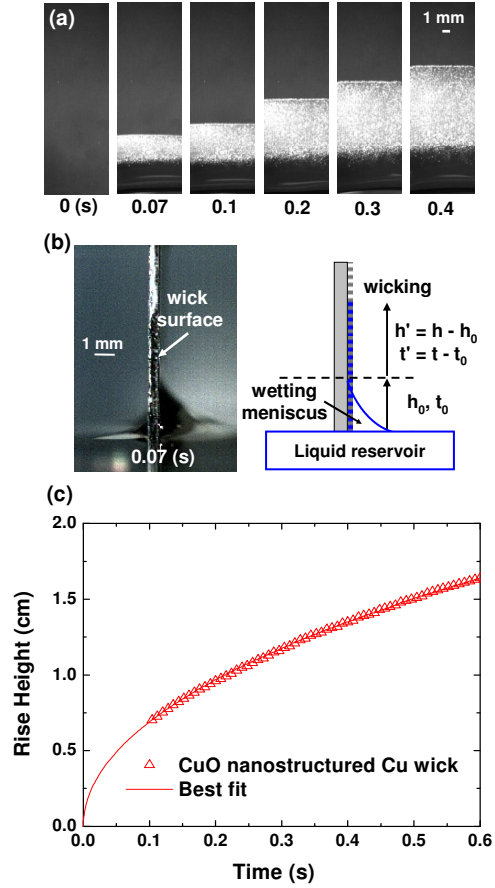


Fig. 5: (a) Selected video frames (front view) from our capillary rate of rise experiment on nanostructured Cu micropost wick (50  $\mu\text{m}$  diameter, 100  $\mu\text{m}$  pitch,  $\sim 110 \mu\text{m}$  height) (b) side view (c) measured rise height as a function of time with the best fit.

where  $\theta_a$  represents the apparent contact angle of the wick surface. The height of the side meniscus ( $h_0$ ) is subtracted from the liquid rise height ( $h$ ) and the associated transient time ( $t_0$ ) from the original measurement time ( $t$ ) in our analysis as illustrated in Fig. 5(b).

The measured liquid rise height is fitted using Eq. (1) to determine the parameters  $K/R_{\text{eff}}$  and  $K$  (Fig. 5(c)). The goodness of fit is evaluated by calculating the mean absolute deviation (M.A.D.) defined as the average value of  $[(t_m - t_c)/t_c]$ , where  $t_m$  = measured value and  $t_c$  = calculated value.

When the gravity effect is relatively weak, which is the case for our 3 cm-long samples, the liquid rise height is a strong function of the ratio  $K/R_{\text{eff}}$  but only a weak function of the individual value of  $K$  or  $R_{\text{eff}}$  (see Washburn's equation, Eq. (2)). Even when we change the value of  $K$  by  $\pm 40\%$  from its best fit value, for example, the M.A.D. changes less than 1%. Such

large uncertainty was overlooked in previous studies. While the accuracy of  $K$  (or  $R_{\text{eff}}$ ) can be improved by using much longer samples, liquid evaporation makes it impractical to track liquid menisci over several cm.

## DISCUSSION

To investigate the effects of the post diameter and pitch on the capillary performance, two sets of samples are fabricated as summarized in Table 1. In case I, the diameter of the post  $D_p$  is fixed at  $50 \mu\text{m}$  and the pitch  $P$  is varied by changing the distance between the nearest neighboring posts. In case II, the distance between the nearest neighboring posts is fixed at  $50 \mu\text{m}$  while the post diameter is varied from  $30 \mu\text{m}$  to  $100 \mu\text{m}$ . All subsequent characterization is performed for posts with height approximately  $100 \mu\text{m}$ , which is deemed optimal from a preliminary heat transfer modeling study.

Table 1: Design parameters of tested micropost wicks

Case	$D_p$ [ $\mu\text{m}$ ]	$D_{\text{cc}}$ [ $\mu\text{m}$ ]	$P$ [ $\mu\text{m}$ ]	$f_s$
I	50	15	65	0.537
		25	75	0.403
		37.5	87.5	0.296
		50	100	0.227
		65	115	0.171
II	30	50	80	0.128
	50		100	0.227
	75		125	0.326
	100		150	0.403

Figure 6 shows the wicking performance ( $K/R_{\text{eff}}$ ) of the micropost wicks presented in Table 1 as a function of solid fraction  $f_s$ . For a given solid fraction, the measured values of  $K/R_{\text{eff}}$  are similar for both cases and decreases approximately linearly with solid fraction, which suggests that  $K/R_{\text{eff}}$  is mainly a function of solid fraction.

## CONCLUSION

Multiscale superhydrophilic Cu micropost arrays are demonstrated using electrochemical deposition combined with a controlled chemical oxidation scheme. The measured wicking performance is primarily a function of solid fraction and decreases approximately linearly with solid fraction.

Our characterization work provides a useful starting point to achieve optimal balance between the wicking performance and the effective wick thermal conductivity. The fabrication process suggested in this study can also be applied to other devices requiring

dense arrays of metallic microposts.

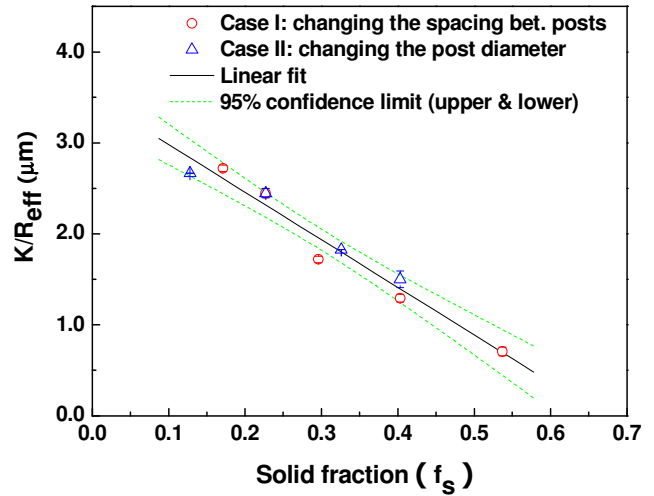


Fig. 6:  $K/R_{\text{eff}}$  of micropost wicks as a function of solid fraction.

## REFERENCE

- [1] G. P. Peterson, Appl. Mech. Rev., 45, 175 (1992).
- [2] C. B. Sobhan, R. L. Rag, and G. P. Peterson, Int. J. Energy Res., 31, 664 (2007).
- [3] W. K. Jones, Y. Liu, and M. Gao, IEEE Trans. on Compon. and Packag. Technol., 26,110 (2003).
- [4] V. K. Dhir, J. Heat Transfer, 128, 1 (2006).
- [5] Y. Takata, S. Hidaka, M. Masuda and T. Ito, Int. J. Energy Res., 27, 111 (2003).
- [6] Z. Liu and Y. Qiu, J. Heat Transfer, 128, 726 (2006).
- [7] H. Makamba, J. H. Kim, K. Lim, N. Park and J. H. Hahn, Electrophoresis, 24, 3607 (2003).
- [8] J. L. Fritz and M. J. Owen, J. Adhesion, 54, 33 (1995).
- [9] N. T. Nguyen, E. Boellaard, N. P. Pham, V. G. Kutchoukov, G. Craciun and P. M. Sarro, J. Micromech. Microeng., 12, 395 (2002).
- [10] P. Dixit and J. Miao, J. Electrochem. Soc., 153, G552 (2006).
- [11] Y. Nam and Y. S. Ju, Proc. IMECE, 2008-67492.
- [12] B. Holley and A. Faghri, Appl. Therm. Eng., 26, 448 (2006).
- [13] N. Fries, K. Odic, M. Conrath and M. Dreyer, J. Colloid Interface Sci., 321, 118 (2008).
- [14] E. W. Washburn, Phys. Rev., 17, 273 (1921).
- [15] P.G. Gennes, F. Brochard-Wyart and D. Quéré, Capillary and Wetting Phenomena, Springer (2004).